DEUTSCHES ELEKTRONEN-SYNCHROTRON DESY

DESY 80/43
May 1980

RESULTS FROM PLUTO

by

H. Spitzer

II. Institut für Experimentalphysik der Universität Hamburg

NOTKESTRASSE 85 · 2 HAMBURG 52

To be sure that your preprints are promptly included in the
HIGH ENERGY PHYSICS INDEX ,
send them to the following address (if possible by air mail) :

DESY
Bibliothek
Notkestrasse 85
2 Hamburg 52
Germany

DESY 80/43
May 1980

RESULTS FROM PLUTO

H. Spitzer
Universität Hamburg
II. Institut für Experimentalphysik
Notkestr. 85, D2000 Hamburg-52

Abstract

Recent results obtained with the PLUTO detector at the e^+e^- storage ring PETRA are reviewed. The validity of QED has been successfully tested in five independent reactions at spacelike momentum transfers up to -850 GeV^2 and timelike momentum transfers up to 1000 GeV^2. We are performing a detailed study of hadron production through 2 γ interactions. In particular we have measured the total hadronic $\gamma\gamma$ cross section and have determined the radiative width of the f^0 meson to be $\Gamma (f \to \gamma\gamma) = (2.3 \pm 0.5 \pm 0.35)$ keV. The first indication for the production of large p_t jets in 2γ interactions is presented. We find no evidence for a $t\bar{t}$ threshold in the rate of inclusive muons. Finally we give a lower limit (95 % c.l.) of 13 GeV on the mass of a spin 0 electron expected from supersymmetry.

Talk given at the XVth Rencontre de Moriond,
Les Arcs, France, March 15-21, 1980

1. Introduction

High energy electron-positron interactions as studied at SPEAR, DORIS and PETRA have turned out to be a rich source of new leptons, flavors (quarks) and bosons. They also provide a clean testing ground for pointlike interactions. In this talk I will report recent results from the PLUTO detector on the following topics:

QED tests (section 2)
2γ interactions (section 3)
Search for new flavors (section 4)
Search for new leptons (section 5)

Results on jet production and QCD tests in one photon annihilation have been discussed in the first weak of this conference by D. Schmidt[1].

The PLUTO detector is operated by a collaboration of eight institutions[2]. Let me summarize the main features of the detector. The central detector consists of 13 cylindrical proportional chambers surrounded by scintillation shower counters. It provides a hadron spectrometer and an electron calorimeter[3]. Forward shower counters down to angles of 1^{o} are used for tagging electrons from 2γ interactions[4]. A one meter iron shield surrounded by drift chambers allows muon identification[5]. The inner shower counters measure also the time of flight of traversing particles which is essential for rejecting cosmic ray muons.

I will report here on data taken at DORIS and PETRA. Table 1 shows the integrated luminosities collected at different energies. In total we obtained a luminosity of 3570 nb^{-1} at center of mass energies from 9.4 to 31.6 GeV.

Table 1 Integrated luminosity collected with the PLUTO detector in 1978 and 1979

E_{cm} (GeV)	Luminosity (nb^{-1})	
9.4 (incl. Υ region)	370	DORIS (1978)
12, 13, 17	250	PETRA (1979)
22, 27.5	450	
30 - 31.6	2500	
	sum 3570	

2. QED tests

The high energies available at PETRA allow QED tests up to timelike momentum transfers of $s = 1000\ GeV^2$ and up to spacelike momentum tranfers of $q^2 = -850\ GeV^2$. This may be compared to the QED tests performed at SPEAR which covered the energy range up to $s = 55\ GeV^2$ [6,7]. Table 2 shows the reactions and the basic QED diagrams which have been studied by the PLUTO group.

Table 2 Basic QED diagrams studied

reaction	lowest order QED diagram	exchanged particle	lowest order contribution from weak interaction
1) ee → ee	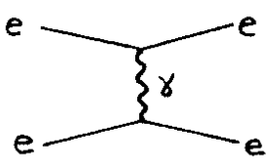	spacelike photon	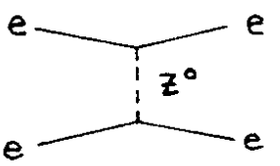
1) ee → ee 2) ee → μμ 3) ee → ττ	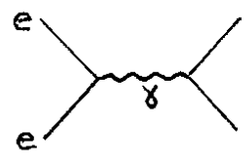	timelike photon	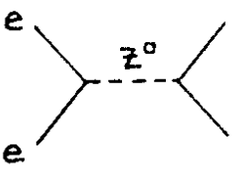
4) ee → γγ	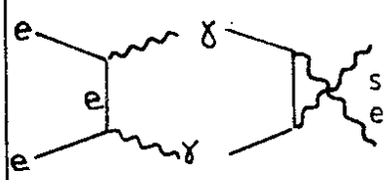	spacelike electron	none
5) ee → eeee → eeμμ	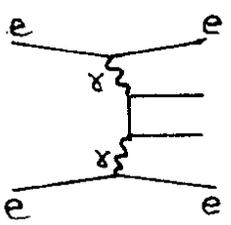	spacelike electron + quasireal γ	

Reactions 1 - 3 are expected to have small contributions from weak interactions via Z^0 exchange. There is no first order weak graph contributing to the reaction ee → γγ. At higher energies this will be the reaction best suited for testing QED.

Note that reaction 5 is dominated by graphs of order α^4, which can be tested here much better than in radiative corrections to reactions 1 - 4.

In the following I want to discuss two questions

- How well does QED decribe the data?
- Can we observe weak interactions effects?

The data were extracted by applying the cuts shown in Table 3. Corrections for inefficiencies have been included.

Table 3 Cuts applied to the QED data

reaction	acceptance	acollinearity angle	minimum particle energy
$e^+e^- \to e^+e^-$	$\lvert\cos\theta\rvert < 0.8$	$< 15^0$	$\geq 0.33\ E_{beam}$
$e^+e^- \to \mu^+\mu^-$	$\lvert\cos\theta\rvert < 0.5$	$< 6^0$	$\geq 0.75\ E_{beam}$
$e^+e^- \to \tau^+\tau^-$	$\lvert\cos\theta\rvert < 0.8$	no cut	charged particles from τ decays: $P_1 > 0.5$ GeV $P_2 > 0.8$ GeV
$e^+e^- \to \gamma\gamma$	$\lvert\cos\theta\rvert < 0.75$	$< 20^0$	$\geq 0.25\ E_{beam}$

Let us first have a look at the integrated reaction cross sections. QED predicts that the cross sections for reactions 1-4 display the characteristic $1/E_{cm}^2$ behaviour of a pointlike process. Figure 1 shows the cross section for reaction ee $\to \gamma\gamma$ measured for $|\cos\theta| < 0.75$ as a function of the center of mass energy E_{cm}. Fig. 2 shows the cross sections for ee $\to \mu\mu$ (circles) and ee $\to \tau\tau$ (squares) integrated over the full angular range ($0 < \theta < 180^0$). The data agree very well with the $1/E_{cm}^2$ behaviour expected from QED.

Possible QED modifications in reactions 2 and 3 are usually parametrized by introducing a form factor into the cross section

$$\left.\frac{d\sigma}{d\Omega}\right|_{exp} = \left.\frac{d\sigma}{d\Omega}\right|_{QED} |F_T(s)|^2\ (1 + \delta_{rad}) \qquad (1)$$

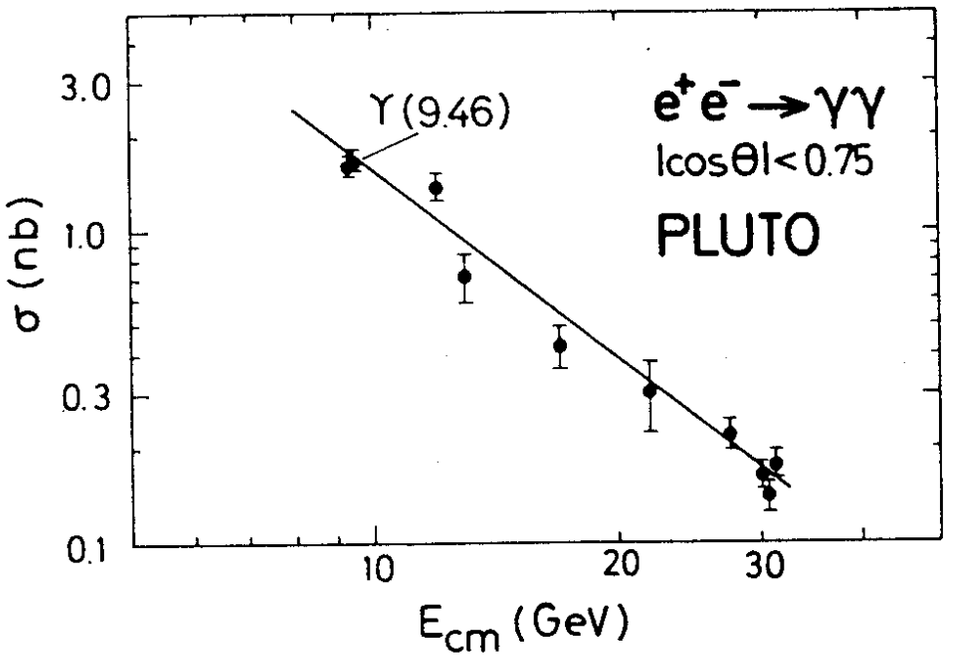

Fig. 1 The cross section for $e^+e^- \to \gamma\gamma$ integrated over the angular region $|\cos\theta| < 0.75$. The full line is the QED expectation including the effects of radiation and angular resolution.

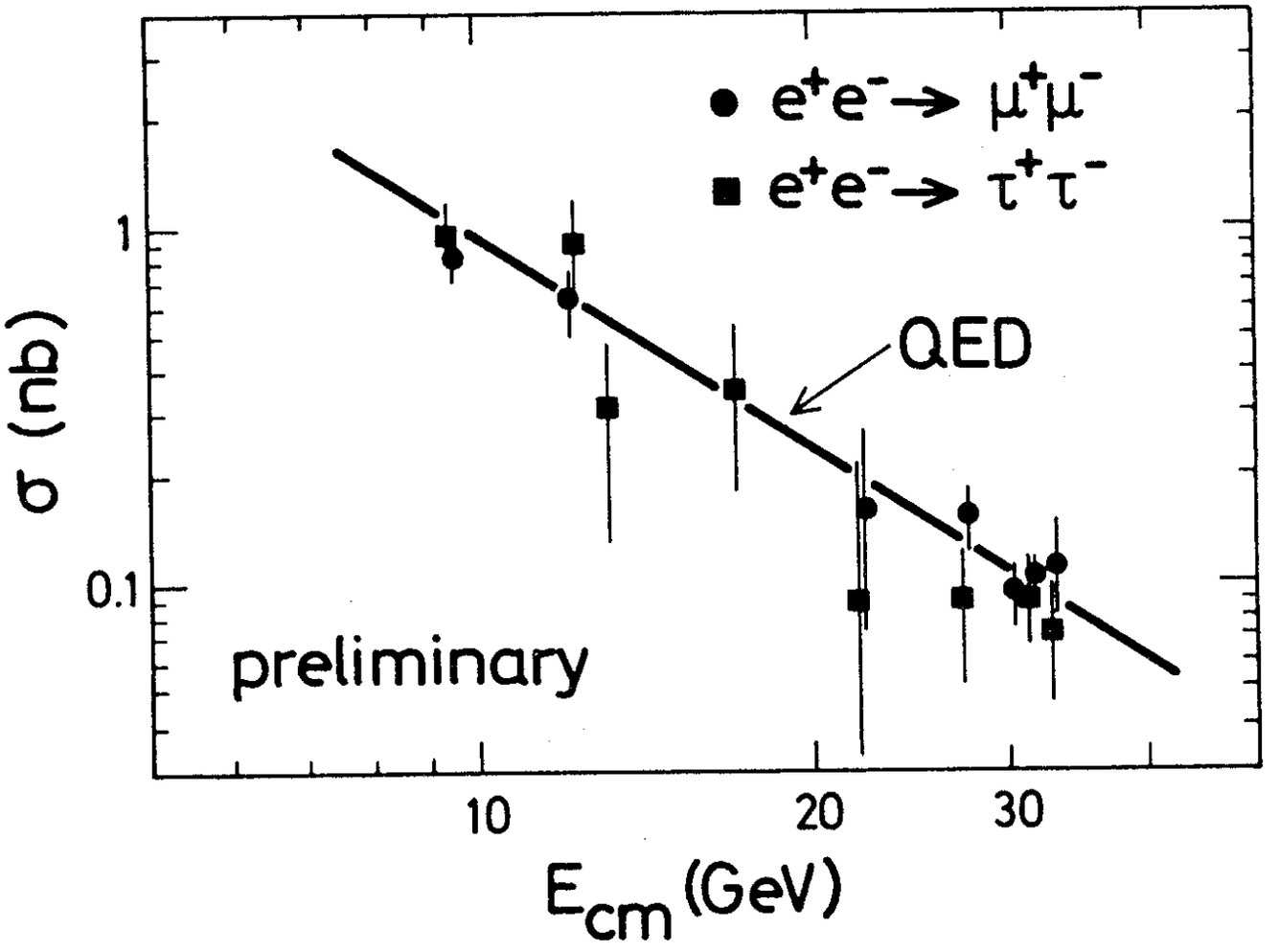

Fig. 2 The total cross section for $e^+e^- \to \mu^+\mu^-$ (circles) and $e^+e^- \to \tau^+\tau^-$ (squares) as a function of E_{cm}. The full line is the expectation from first order QED.

Here δ_{rad} is the radiative correction. It is obvious from Fig. 2 that $F_T(s) \simeq 1$. Hence we expand

$$F_T(s) = 1 \pm \frac{s}{\Lambda_{T\pm}^2} \quad . \qquad (2)$$

The plus and minus signs correspond to different ways of formulating a modified QED[8]. The Λ's are referred to as cutoff parameters. The values of Λ^2 were obtained from a fit of eq. (1) to the data, where the fit selected the sign in eq. (2) required to describe the data. The errors of the fitted parameters allow the derivation of lower limits on both Λ_+ and Λ_-. The results are given in Table 4.

Table 4 Fitted values of $1/\Lambda^2$ and lower limits on the QED cutoff parameters (95 % c.l.)

reaction	parametrization	$1/\Lambda^2$ (GeV^{-2})	Λ_+ (GeV)	Λ_- (GeV)
$e^+e^- \to e^+e^-$	$F_S = 1 \pm q^2/\Lambda_{S\pm}^2$	$0.000110^{+0.000064}_{-0.000069}$	≥ 71	≥ 250
(ref. 3)	$F_T = 1 \pm s/\Lambda_{T\pm}^2$	$0.000003^{+0.000145}_{-0.000150}$	≥ 71	≥ 78
	$F_S = F_T$	$0.000085^{+0.000054}_{-0.000058}$	≥ 80	≥ 234
$e^+e^- \to \mu^+\mu^-$ (preliminary)	$F_T = 1 \pm s/\Lambda_{T\pm}^2$	0.000019 ± 0.000052	≥ 87	≥ 99
$e^+e^- \to \tau^+\tau^-$ (preliminary)	$F_T = 1 \pm s/\Lambda_{T\pm}^2$	-0.00016 ± 0.00017	≥ 74	≥ 65
$e^+e^- \to \gamma\gamma$	$F_V(q) = 1 \pm q^4/\Lambda_{V\pm}^4$	$s^2/\Lambda_V^4 = -0.169 \pm 0.185$	≥ 46	≥ 36
(ref. 9)	$F_V(q') = 1 \pm q'^4/\Lambda_{V\pm}^4$			
	heavy electron	$s^2/\Lambda_e^4{}^* = -0.083 \pm 0.145$	≥ 46	

Let us next look at differential cross sections. Fig. 3a and b show the differential cross section for Bhabha scattering measured from $\cos\theta = -0.8$ to $\cos\theta = +0.8$ at $E_{cm} = 9.4$ GeV and $E_{cm} = 30$ GeV. The curve is the QED cross section including the effects of radiation and the finite angular resolution of the detector[3]. The predictions agree well with the data.

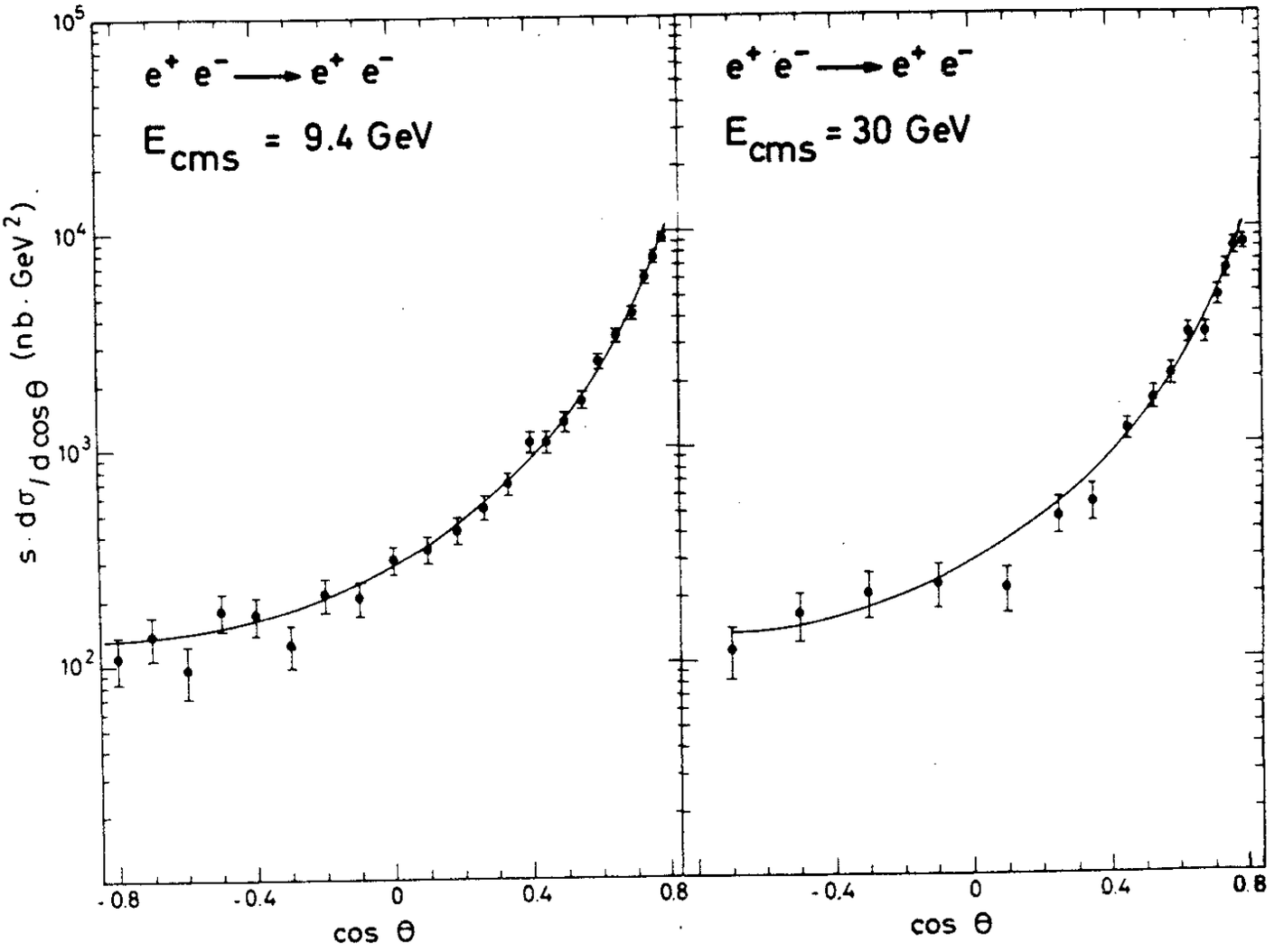

Fig. 3 The differential cross section s dσ/d cosθ for Bhabha scattering at cms energies of (a) 9.4 and (b) 30 GeV. The curves are the QED cross sections including the effects of radiation and angular resolution.

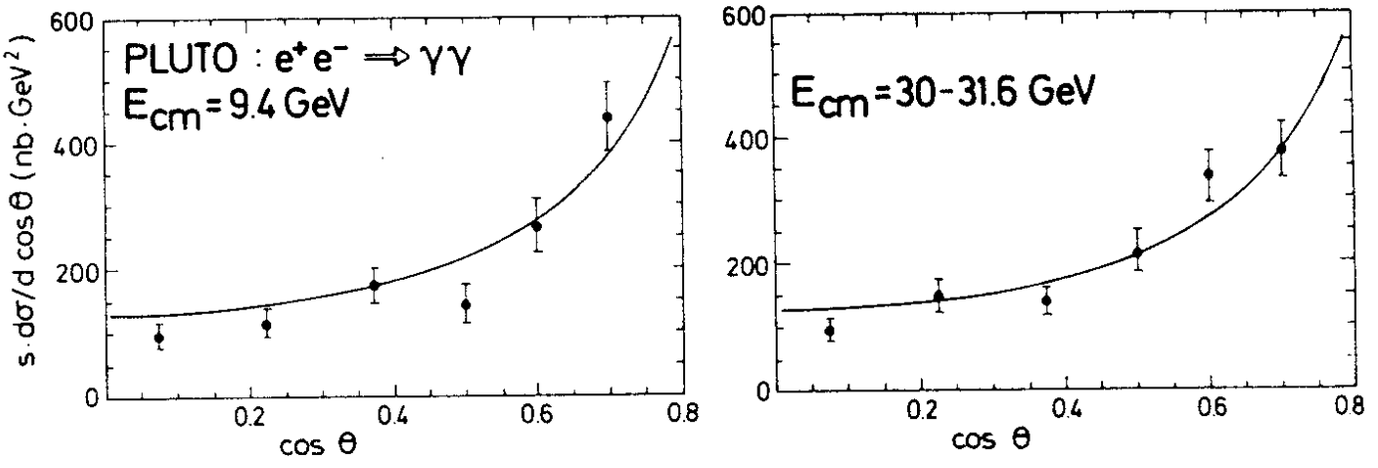

Fig. 4 The differential cross section s dσ/d cosθ for the reaction ee → γγ. The curve is the QED prediction including radiative effects and angular resolution.

Possible QED modifications have been parametrized by introducing the form factor eq.(2) into the timelike amplitude and by introducing a second form factor

$$F_S(q^2) = 1 \pm \frac{q^2}{\Lambda_{S\pm}^2} \qquad (3)$$

into the spacelike amplitude for Bhabha scattering. The resulting lower limits on the Λ's derived from a fit to the data[3] are given in Table 4. We attribute the difference between the lower limits on Λ_+ and Λ_- to a statistical fluctation or an unresolved systematic effect. Fig. 4 shows the differential cross section for the reaction $e^+e^- \to \gamma\gamma$ at 9.4 GeV and in the energy range $30 \leq E_{cm} \leq 31.6$ GeV. The curve is the QED prediction including radiative effects (of the order 0 - 3 % depending on the angle) and the angular resolution. Good agreement is found.

We have applied two possible modifications of the standard QED cross section, which have been suggested in the literature:

- based on a vertex modification (sea-gull graph[8c]) the differential cross section can be written as

$$\frac{d\sigma_V}{d\Omega} = \frac{\alpha^2}{2s}\left\{\frac{q'^2}{q^2}\,|F(q^2)|^2 + \frac{q^2}{q'^2}\,|F(q'^2)|^2\right\}(1 + \delta_{rad}) \qquad (4)$$

with $F(q^2) = 1 \pm \frac{q^4}{\Lambda_{V\pm}^4}$, $F(q'^2) = 1 \pm \frac{q'^4}{\Lambda_{V\pm}^4}$

and $q^2 = -s\cos^2\theta/2$ and $q'^2 = -s\sin^2\theta/2$.

- on the other hand, if one assumes the exchange of a hypothetical heavy electron e^*[10] then:

$$\frac{d\sigma_{e^*}}{d\Omega} = \frac{\alpha^2}{2s}\left\{\frac{q'^2}{q^2} + \frac{q^2}{q'^2} \pm \frac{2s^2 - 4q^2q'^2}{\Lambda_{e^*\pm}^4}\right\}(1 + \delta_{rad})$$

The value of Λ_{e^*+} can be interpreted as the mass of a heavy electron assuming its coupling strength is the same as that of the electron. The parameter Λ_{e^*-} is theoretically less motivated. In both cases the relative modification is largest and of same magnitude at $\theta = 90^0$.

Both expressions were fitted to the experimental differential cross sections at $30 \leq E_{cm} \leq 31.6$ GeV. Lower bounds for the cutoff parameters Λ_{V+}, Λ_{V-}, $\Lambda_{e}*$ were obtained as shown in Table 4.

The fitted values of $1/\Lambda^2$ and s^2/Λ^4 from reactions 1-4 are consistent with zero and thus show good agreement with QED. These results and the comparable measurements of the other PETRA experiments (JADE, MARK J and TASSO) demonstrate the continued strength of QED in describing the interactions of leptons and photons up to the highest energies reached so far.

Next we have measured the angular distribution of μ-pairs in the process $ee \to \mu\mu$, as shown in Fig. 5. From weak interference effects one would expect a forward-backward asymmetry of -5 %, whereas radiative corrections should lead to an asymmetry of +1.5 %. The observed asymmetry is (+6.8 ± 8.9) %. It is obvious that weak interaction effects cannot be established with the present data. However one can use the Bhabha and muon data to derive limits on parameters of the Weinberg - Salam model. Work along those lines is underway.

Let me finally discuss a QED test in 2γ processes. We have measured the reactions

$$\text{and} \quad \begin{matrix} ee \to ee\ ee \\ ee \to ee\ \mu\mu \end{matrix} \qquad (5)$$

by detecting events with two tracks in the inner detector and one electron tagged in the forward shower counter. The average Q^2 of one of the virtual photons is $Q^2 \simeq 0.25$ GeV^2, whereas the other photon has $Q^2 \simeq 0$. The tracks in the inner detector are dominantly electrons and muons with an estimated pion contamination of about 15 %. Fig. 6 shows the invariant mass distribution of the two tracks in the inner detector. The curve is the absolute QED prediction from a program of J. Vermaseren[11]. This program includes an exact calculation of reaction (5) together with its interference with bremsstrahlungsterms ($ee \to ee\ \gamma \hookrightarrow ee$). The QED curve agrees well with the data within their systematic uncertainty of 15 %. Radiative corrections to the 2γ process have not yet been included and are expected to partly cancel the π contribution. Thus QED seems to work well in a process dominated by α^4 contributions at low Q^2.

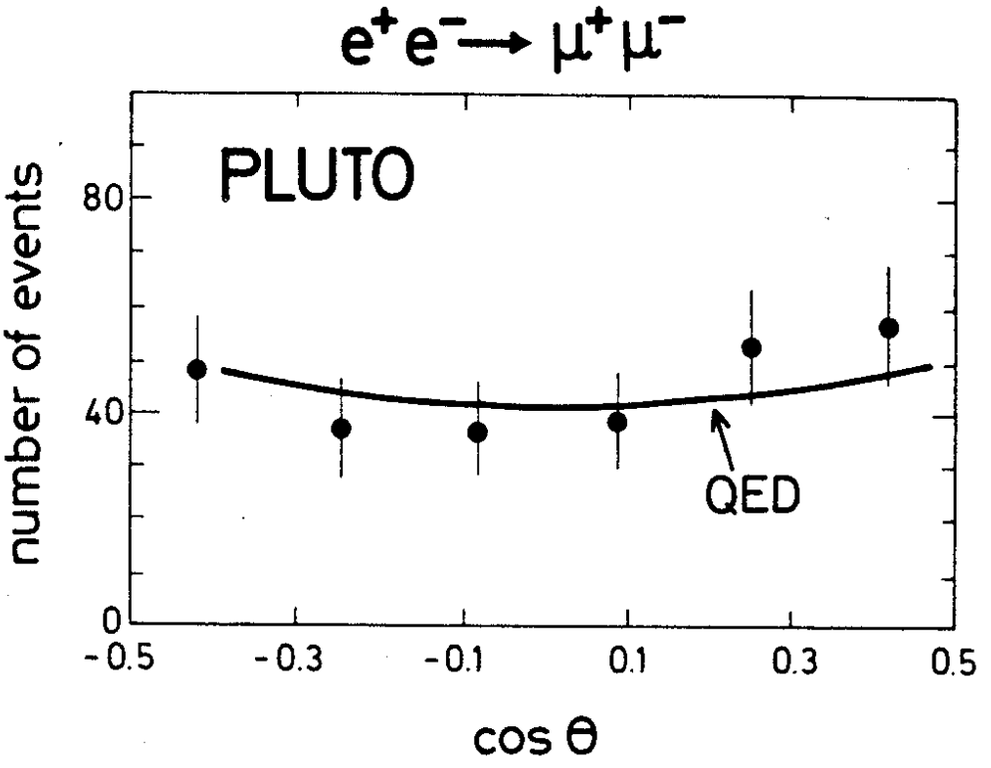

Fig. 5 The angular distribution of the reaction $e^+e^- \rightarrow \mu^+\mu^-$ for $22 < E_{cm} < 31.6$ GeV. The curve is the first order QED prediction.

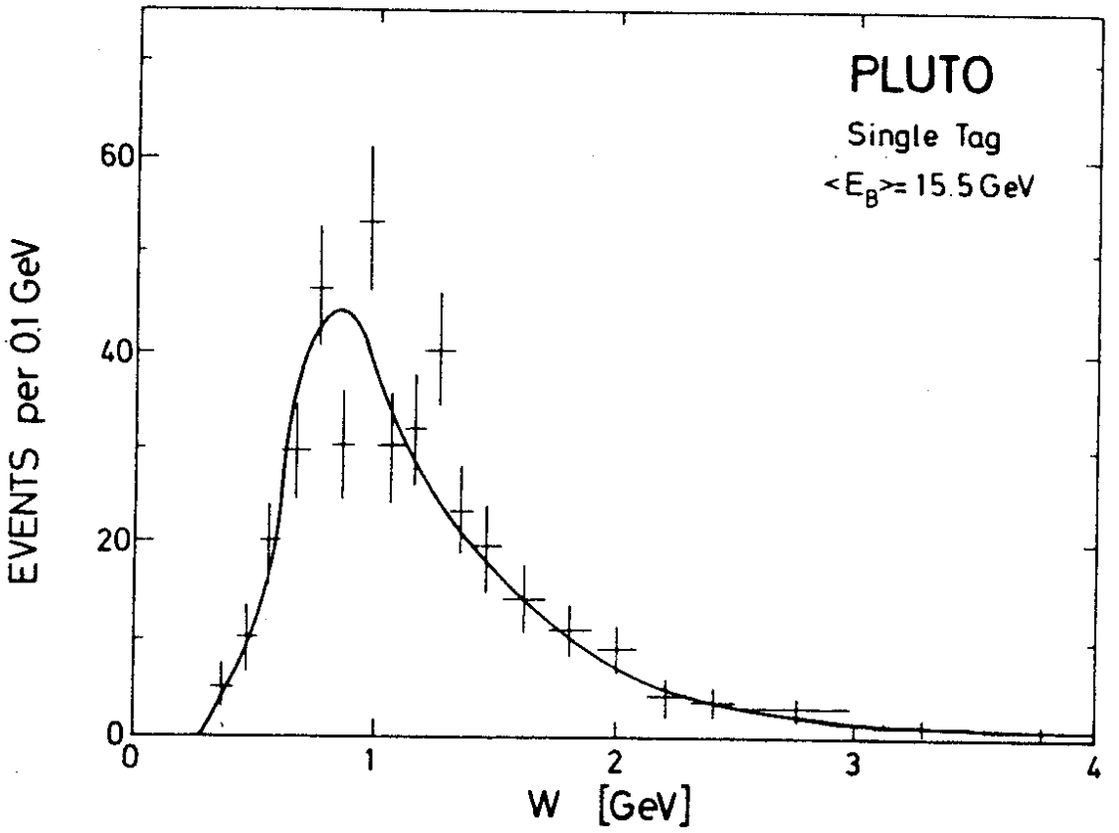

Fig. 6 The effective two particle mass W from reaction ee → ee 2prongs, where the 2 prongs had production angles $\theta > 56^\circ$ and $p_t > 400$ MeV. For technical reasons we assigned pion masses to the particles when computing W. The curve is from an absolute QED calculation.

3. Hadron production in $\gamma\gamma$ interactions

3.1. Introduction

The scattering of light by light is a process expected from quantum electrodynamics which cannot occur in the classical framework of linear Maxwell equations. Two photon interactions in e^+e^- reactions probe the scattering of virtual and quasireal photons. With the present PLUTO detector we can study two different kinematic configurations[12]:

a) Single tagging

The basic diagram is as follows

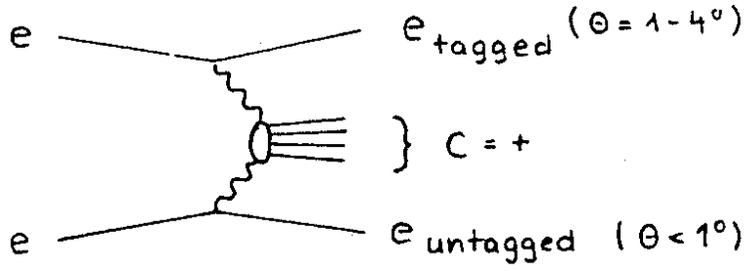

One of the scattered electrons is tagged at an angle between 1^0 and 4^0 (later up to 15^0) resulting in an average Q^2 of 0.25 GeV^2 for the data taken at E_{beam} = 15 - 16 GeV. The other photon has $Q^2 \approx 0$. The process can be considered as electroproduction on a quasireal photon[4]. The cross section has two terms $\sigma_T + \varepsilon\sigma_L$.

b) No tagging

In this configuration both electrons are scattered at angles less than one degree and both photons have $Q^2 \approx 0$. Here we measure the scattering of two quasireal photons. The cross section has one term only[12].

Events from $\gamma\gamma$ interactions present a clear signature. Since the $\gamma\gamma$ center of mass system generally has much less energy than the overall e^+e^- cms, we expect events with little energy in the central detector. This is illustrated in Fig. 7, where the total energy observed in the central detector is plotted. A clean separation between events from 1γ and 2γ processes is possible. In the following I will discuss three topics: the production of f^0 mesons, the total cross section for hadron production and the first indications for large p_t jets in 2γ processes.

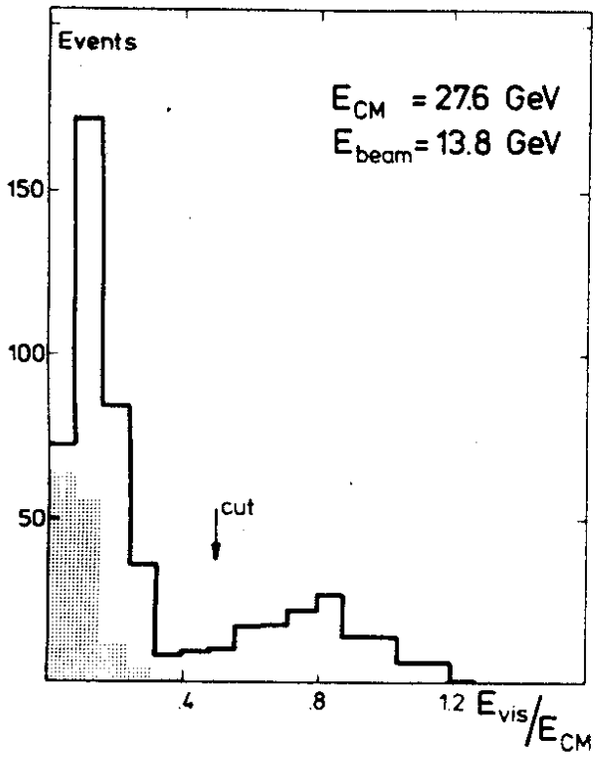

Fig. 7 The total energy observed in the central detector divided by E_{cm} at a beam energy of 13.8 GeV. A beam gas subtraction has been performed. The shaded events are from single tag data.

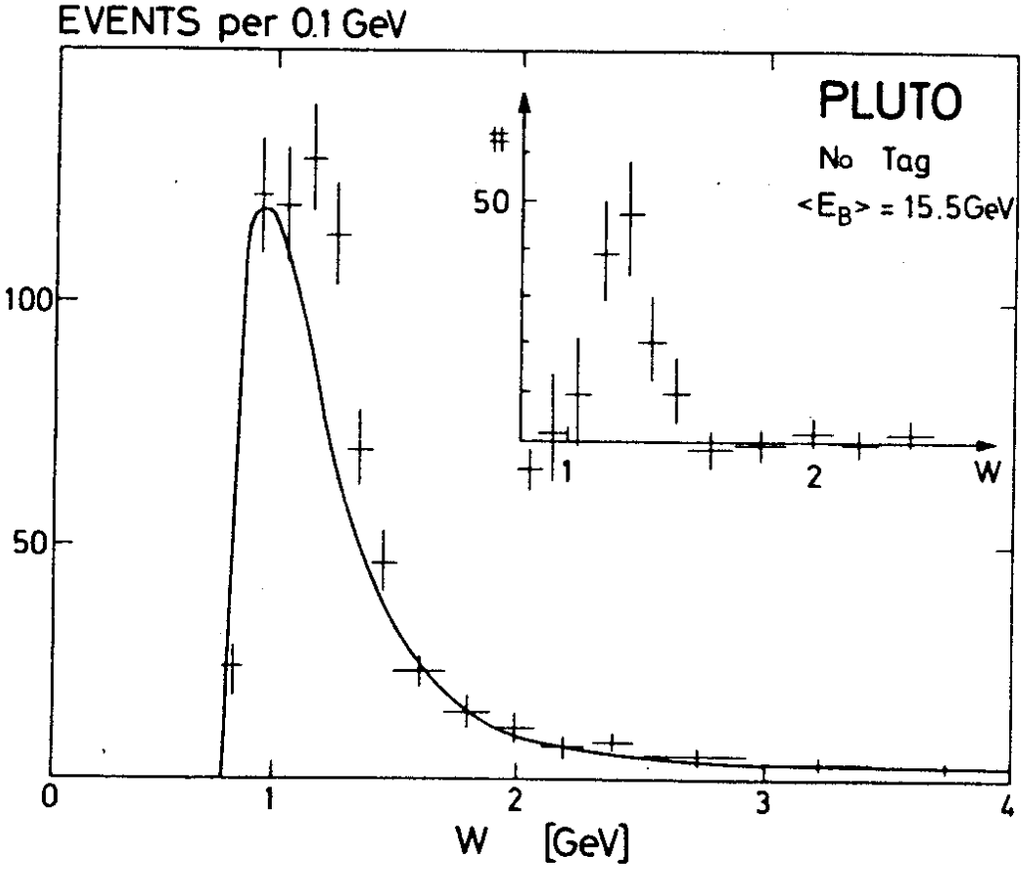

Fig. 8 The effective mass of the 2prongs from reaction ee → ee 2prongs. The curve is an absolute QED prediction. The insert shows the difference between data and QED background in the f^0 region.

$N(k_1)$ and $N(k_2)$ are flux factors for quasireal photons of energy k_1 and k_2. The decay angular distribution of the f^0 was chosen to be of the form $P(\theta_{cm}) \sim \sin^4\theta_{cm}$; i.e. we assume dominance of helicity 2 amplitudes[14].

The resulting value of the radiative width is

$$\Gamma(f \to \gamma\gamma) = 2.3 \pm 0.5 \text{ (statist.)} \pm 0.35 \text{ (syst.)} \text{ at}$$

$$\langle Q_{\gamma_1}^2 \rangle \,, \langle Q_{\gamma_2}^2 \rangle = 0.0065 \text{ GeV}^2.$$

Radiative corrections have not yet been applied, but are expected to be small compared to the systematic error of 15 %.

The experimental result is to be compared with the theoretical predictions, which are listed in table 5. Our result is close to the value obtained in calculations using the nonrelativistic quark model with an oscillator potential[16,17]. With the exception of ref. 14 all methods based on finite energy sum rules, tensor meson dominance etc. lead to larger values for $\Gamma_{\gamma\gamma}$. It should be noted also, that tentatively assuming the helicity zero hypothesis we find $\Gamma_{\gamma\gamma}$ = 5.7 ± 1.3 keV.

Table 5 Measurements and predictions for the radiative width of the $f^0(1270)$

Ref.	$\langle Q_{\gamma_1}^2 \rangle$ (GeV^2)	$\langle Q_{\gamma_2}^2 \rangle$ (GeV^2)	$\Gamma(f^0 \to \gamma\gamma)$ (keV)
This.exp	0.007	0.007	2.3 ± 0.5 ± 0.35
"	0.28	0.007	< 2.6 (95 % c.l.)
14	0	0	0.8
15			> 1
16			1.2 - 2.3
17			2.6
18			5.07
19			7
20			5.7
21			8
22			8
23			9.2
24			11.3
25			21±6
26			28

Finally we have analyzed the much smaller data sample with the single-tag condition, i.e. an electron (positron) scattered into one of the small-angle taggers of the forward spectrometers[4].

The invariant mass distribution has been shown in fig. 6 along with the QED prediction. The small enhancement in the f^0 mass region can be attributed to f^0 production via one almost real (as above) and one virtual ($\langle Q^2 \rangle = 0.28$ GeV^2) photon. Due to the limited statistics we only give an upper limit of $\Gamma_{\gamma^*\gamma} < 2.6$ keV (95 % confidence level) again using the helicity two hypothesis. For extracting this radiative width the flux factor for the virtual photons radiated from the electron scattered into the SAT was taken from the $e\gamma$ scattering formalism described in ref. 4.

3.3 The total cross section for multihadron production

Two photon interactions produce a continuum of hadronic final states. It is a prime objective to determine the size of the hadronic cross section and to study its Q^2 and W dependence. The PLUTO group has measured cross sections in the single tagging mode ($1^0 < \theta_e < 4^0$) equivalent to studying $e\gamma$ scattering at moderate four momentum transfers (Q^2 up to 0.5 GeV^2). First results at $\langle Q^2 \rangle = 0.1$ GeV^2 have been reported a year ago at this conference[27] and have been subsequently published[4]. I will report new data taken at higher Q^2.

Let me first discuss the expected qualitative features of the cross section. The basic diagrams are as follows:

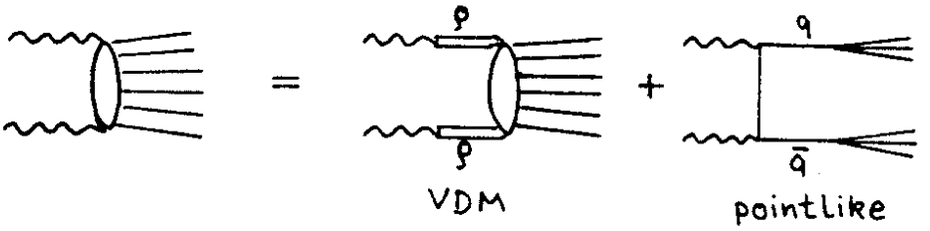

The bulk of the low Q^2 cross section will consist of a VDM type contribution. However we also expect pointlike contributions, where each photon couples to a quark which subsequently fragments into hadrons[28]. The energy dependence of the two contributions to the total cross section can be estimated from the imaginary parts of the related elastic scattering amplitudes. Here the following diagrams contribute:

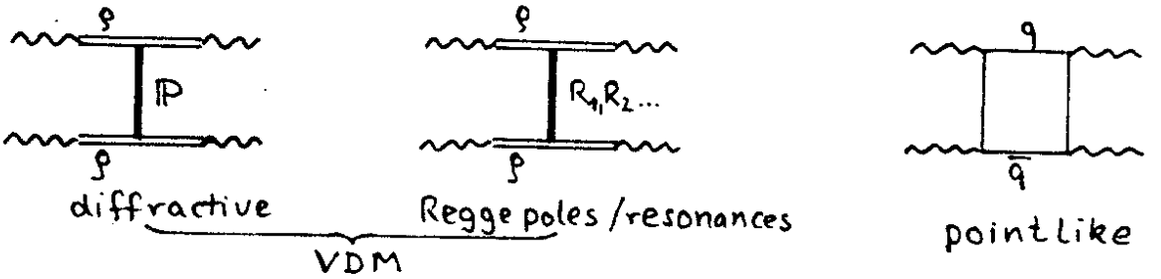

The VDM amplitude has contributions from Pomeron and Regge pole exchanges; the latter ones are dual with s-channel resonances. From factorization we expect that the diffractive term leads to an approximately constant cross section

$$\sigma_{\gamma\gamma}^{\text{diff}} = \frac{\sigma_{\gamma p}^2}{\sigma_{pp}} \approx 240 \text{ nb},$$

where asymptotic values of $\sigma_{\gamma p}$ and σ_{pp} have been used. Regge models predict a decrease of the cross section with rising cm energy W[29]:

$$\sigma_{\gamma\gamma}^{\text{Regge}} \approx \frac{270 \text{ nb GeV}}{W}.$$

Here only the contribution of the leading trajectory was taken into account. Since the q^2 value of one of the photons varies, a ρ propagator term has to be included. Hence we expect:

$$\sigma_{\gamma\gamma}^{\text{diff}} + \sigma_{\gamma\gamma}^{\text{Regge}} = (240 \text{ nb} + \frac{270 \text{ nb GeV}}{W})(\frac{1}{1+Q^2/m_\rho^2})^2. \quad (7)$$

The pointlike coupling can contribute to $\sigma_{\gamma\gamma}$ via a quark box diagram[30]. Its magnitude can be estimated very roughly by

$$\sigma_{\gamma\gamma} = \frac{4\pi\alpha^2}{W^2} \sum_{\substack{\text{color} \\ \text{flavor}}} q_i^4 \ln \frac{W^2}{m_q^2}, \quad (8)$$

where m_q is the quark mass. The pointlike cross section has the typical $1/W^2$ behaviour. As a caution it should be noted that eq.(8) does not include higher order gluonic corrections.

For the cross section determination hadronic events were selected by requiring

a) three or more tracks in the central detector, or
b) two tracks in the central detector and at least one shower which is not associated with the tracks ($E_{\text{neutral}} > 350$ MeV, $|\cos\theta^n| < 0.997$)[4].

The detection efficiency was calculated by a Monte Carlo program which simulated the electron photon scattering process in the PLUTO detector. For the hadronic part of the cross section, $\sigma_T + \varepsilon\sigma_L$, we used a multipion phase space model with constant event rate, independent of Q^2 and W. The transverse momentum distribution was chosen in order to reproduce the observed distribution (fig. 11). The charged multiplicity was taken from low energy e^+e^- annihilation experiments, $n_{ch} = 2+0.7 \ln W^2$. The ratio of charged to neutral pions was taken to be 2 : 1.

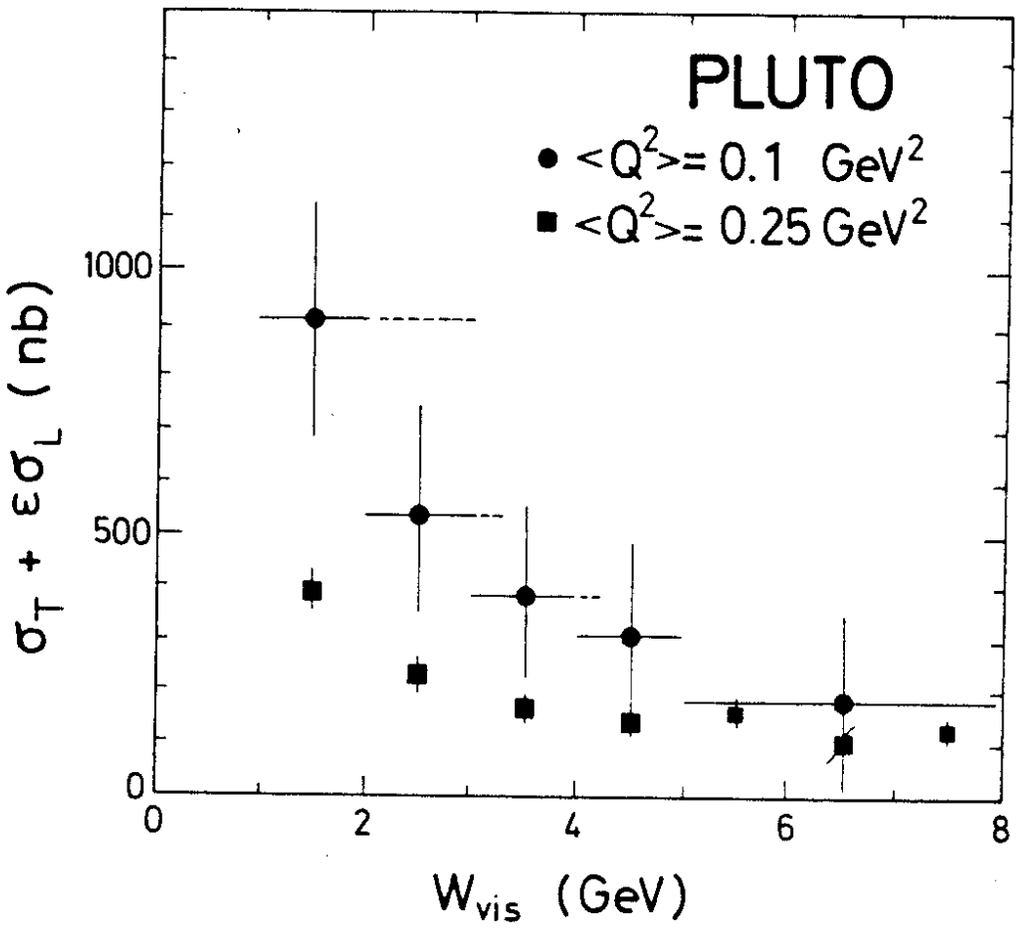

Fig. 9

$\sigma_T + \varepsilon\sigma_L$ vs. W_{vis} for $\gamma\gamma \to \geq 3$ hadrons at $\langle Q^2_{\gamma 1} \rangle \approx 0.1$ GeV^2 and $\langle Q^2_{\gamma 2} \rangle \approx 0.25$ GeV^2. The dashed part of the error bars indicates the range of W that contributes the data point.

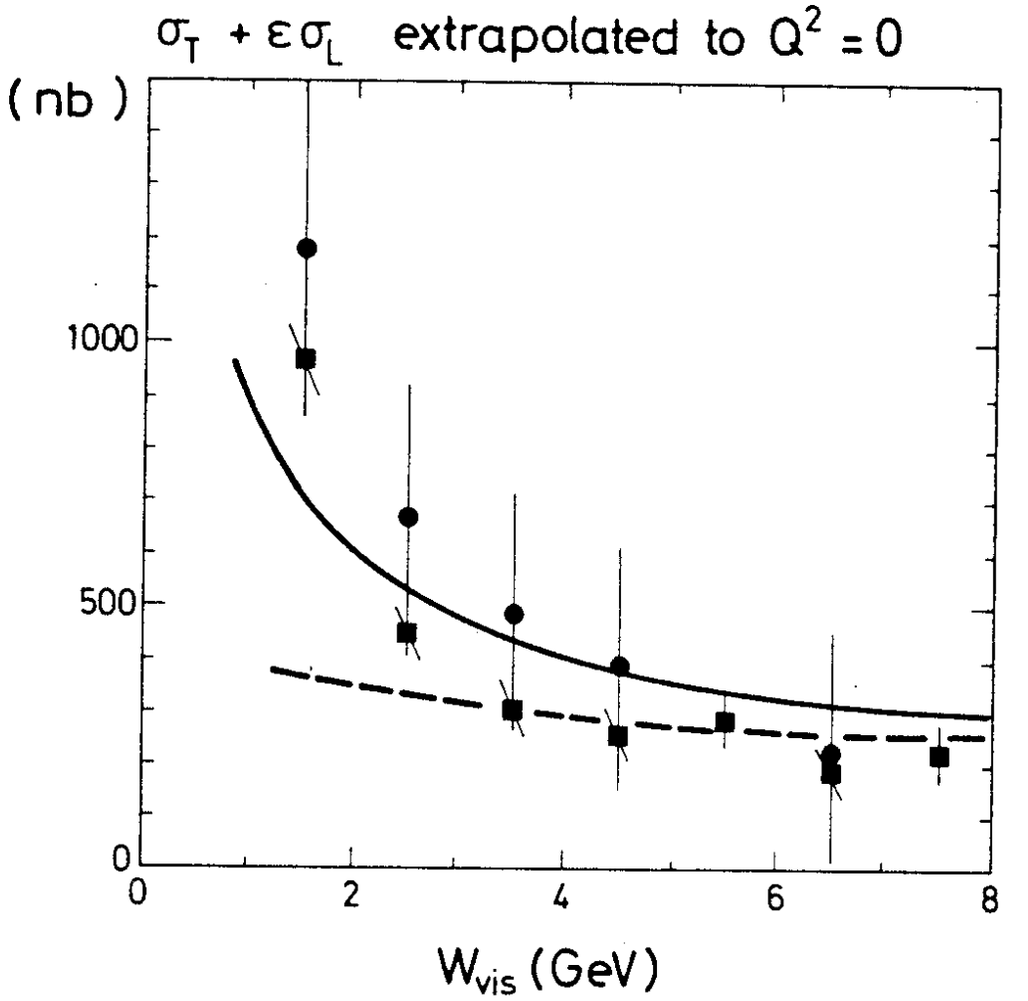

Fig. 10

$\sigma_T + \varepsilon\sigma_L$ from fig. 9 extrapolated to $Q^2 = 0$. The dashed curve is the expected VDM contribution (eq.8). The full curve includes the pointlike contributions (eq.9) for $m_q = 300$ MeV.

Fig. 9 shows the resulting cross section measured at beam energies of 6.5 and 8.5 GeV and $\langle Q_{\gamma 1}^2 \rangle$ = 0.1 GeV^2 (full points[4]). The squares in fig. 9 are recent results from a high statistics run at beam energies of 15.5 GeV and $\langle Q_{\gamma 1}^2 \rangle \approx 0.25$ GeV^2. The cross sections are plotted versus W_{vis}, where W_{vis} is the sum of the charged and neutral energy observed in the central detector assuming pion masses for all particles. The range of true W that contributes to each bin of W_{vis} is indicated by the dashed horizontal bars of the data points. Besides the statistical errors shown we estimate an overall systematic error in the measured cross section of ± 25 %, mainly coming from the uncertainty in the acceptance calculation.

The cross sections have a maximum at low energies and level off for $W_{vis} > 4$ GeV. In order to estimate the hadronic cross section of two real photons we have extrapolated the two sets of data to $Q^2 = 0$ assuming a Q^2 dependence according to the ρ form factor. The results are shown in fig. 10. The dashed curve represents the expected VDM contribution from eq.(7) which has been calculated with a realistic detector simulation. Obviously the VDM contribution can account for the extrapolated cross section above W_{vis} of 3 GeV. The full curve includes the pointlike contribution of eq.(8) assuming a quark mass m_q = 300 MeV. It qualitatively reproduces the rise at the lower energies. Inserting lower quark masses would improve the agreement. However, there is considerable theoretical uncertainty due to the neglect of higher order corrections.

In conclusion: The hadronic cross section above cms energies of 3 GeV is consistent with VDM expectations. The photon seems to interact dominantly like a hadron, but there is room for pointlike contributions. This is illustrated in fig. 11, where we show the p_t^2 distribution of charged particles from multihadron events. We have combined the single tag and the no tag data. The distribution has two distinct contributions, one falling like $\exp(-5\ p_t^2)$ and the other consistent with $\exp(-p_t^2)$ or a p_t^{-4} behaviour. The latter form is indicative of inelastic pointlike collisions. We are presently performing a quantitative analysis by comparing the data to specific models.

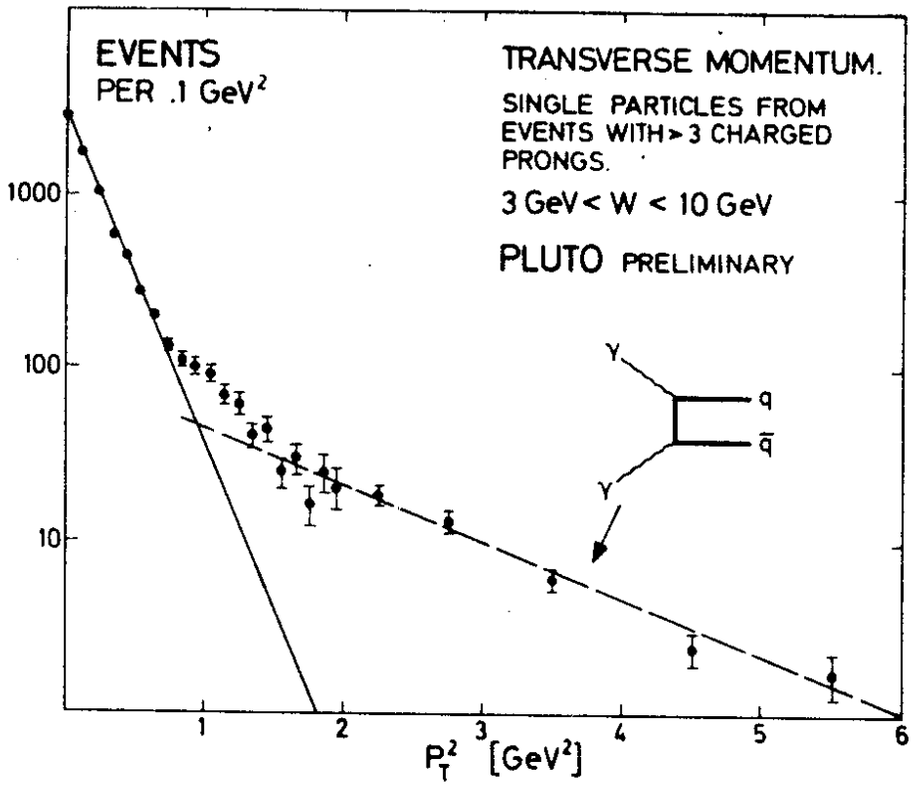

Fig. 11

p_t^2 distribution of charged tracks from 2γ multihadron events for $3 < W_{vis} < 10$ GeV

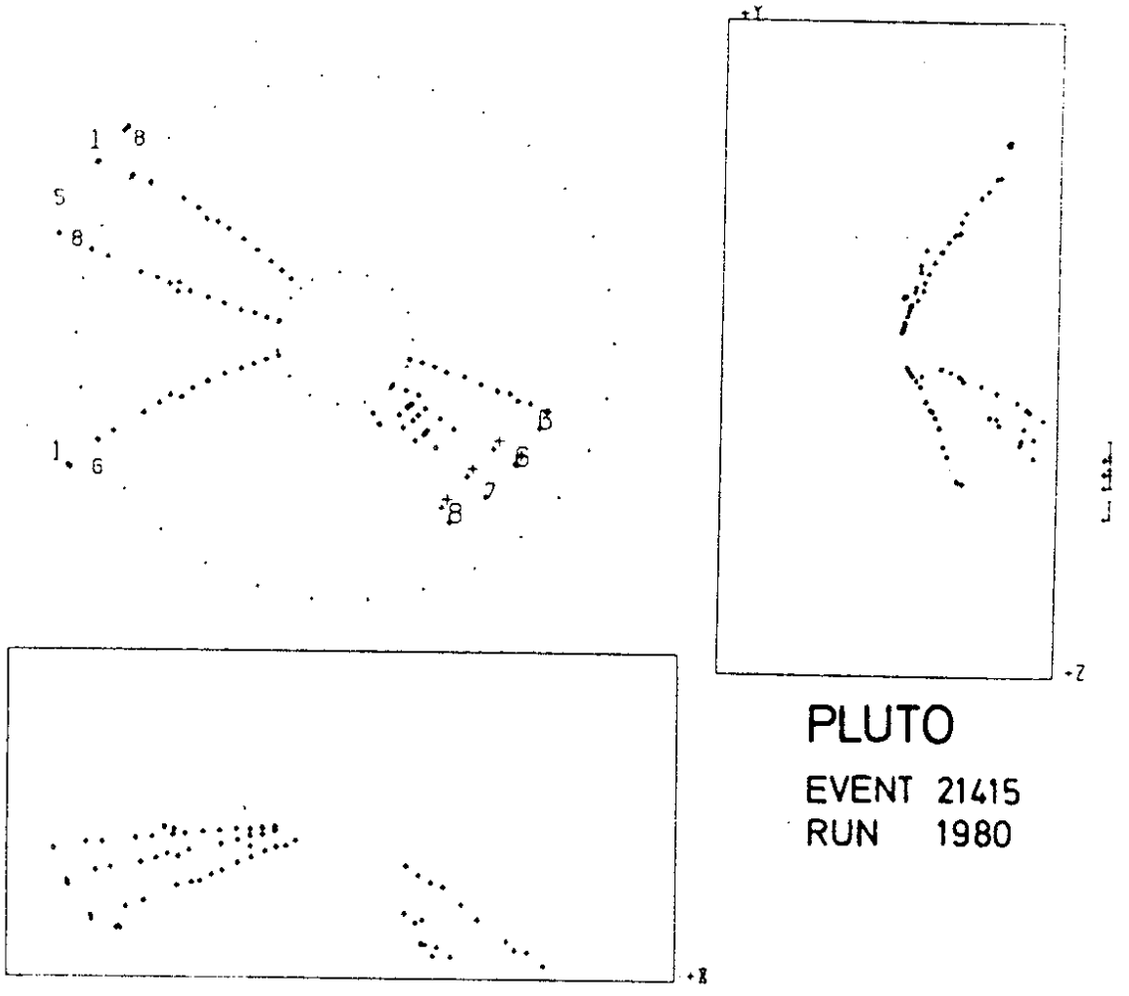

Fig. 12 Candidate for an event of the type ee → ee $q\bar{q}$ seen from three different perpendicular views

3.4 The process $\gamma\gamma \to$ large p_t jets

The question of large p_t jets leads us into the domain of QCD. Last year measurements of one photon annihilation yielded evidence for three jet events[31] which are well described by a pointlike coupling of real gluons to quarks

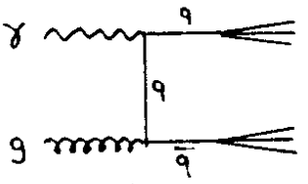

We may ask: can we analogously observe the pointlike coupling of quasireal photons to quarks?

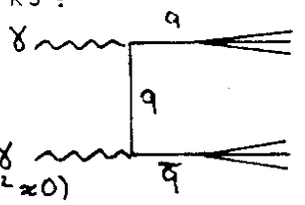

The pointlike photon coupling to quarks should be seen best when the quarks are asymptotically free. I.e. we expect effects when $\alpha_s = \alpha_s(p_{rel}^2)$ becomes small, where p_{rel} is the relative momentum between the two quarks. Small values of α_s imply large values of p_{rel} and p_t, the transverse momentum of the quark relative to the beam axis. The signature of the pointlike photon quark coupling are two non-collinear jets plus some energy from the scattered electrons but no beam pipe jets

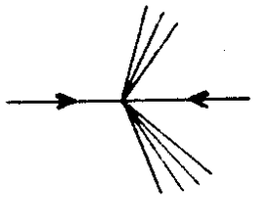

In contrast, large p_t jets from VDM type collisions should be acompanied by two beam pipe jets from the following diagram (as in pp collisions).

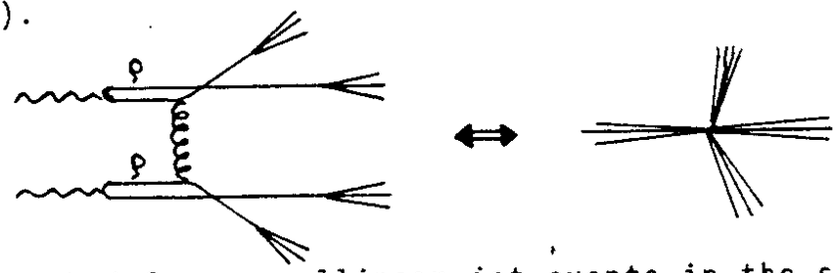

We have searched for noncollinear jet events in the single tag data taken at E_{beam} = 15 - 16 GeV. Fig. 12 shows a typical example. The quantitative analysis included the followings steps:

a) Select events with $\geq$ 4 tracks in total and $\geq$ 2 tracks/jet.

b) Find two noncollinear jets by maximizing the 'Twoplicity' of charged tracks. This variable has been suggested by L. Boesten[32].

It is a thrust quantity allowing for kinked axes.

c) Select events with p_{t_1}, $p_{t_2} > 1.25$ GeV

$$\theta_1 > 51^0, \quad \theta_2 > 36^0$$

$$4 < W_{vis} < 10 \text{ GeV}.$$

$p_{t_{1,2}}$ and $\theta_{1,2}$ are the transverse momenta and polar angles of the two jets relative to the e^+e^- beam axis.

We find a signal of seven events. This signal should be compared to the rate of events from reaction (5) ee → ee ee($\mu\mu$) with the same cuts.

The predicted rate for large p_t jets is[28)]

$$R_{\gamma\gamma \to qq} = \frac{\sigma_{ee \to eeqq}}{\sigma_{ee \to ee\mu\mu}} \approx \sum_{\substack{\text{color} \\ \text{flavor}}} Q_i^4 = \frac{34}{27} \text{ (including charm quarks)}$$

In addition higher order QCD corrections have to be considered. The results are shown in table 6.

Table 6 Number of large p_t jet events and large p_t QED events as compared to the QED prediction[11)].

final state	observed events	expected events (MC)
ee qq	7	
ee $\mu\mu$	4	5.5
ee ee	5	5.5

We find good agreement with the expectation. The events in table 6 result from 50 % of the statistics. The full statistics shows the same trend. Backgrounds from beam gas events and radiative 1γ annihilation events are small. The latter background leads to topologies, where the radiated photon hits the tagging counter opposite to the direction of the two jets. In addition the radiative events are peaked at W > 10 GeV.

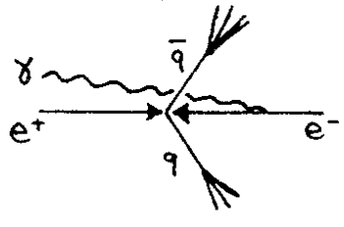

corresponding topology:

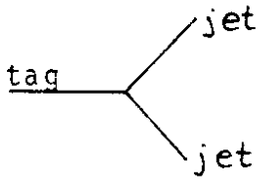

In contrast our data sample in table 6 is restricted to $W < 10$ GeV and has equal number of topologies

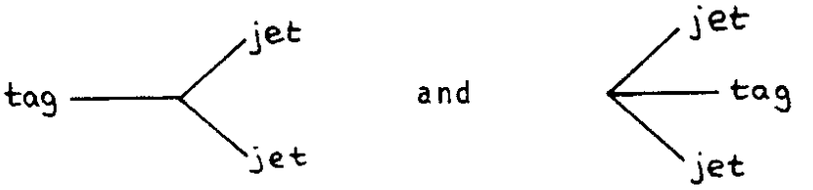

Hence the data are well consistent with the observation of large p_t jets from $\gamma\gamma$ interactions. We finally show in fig. 13 the transverse momentum distribution of the observed charged particles with respect to the jet axis. The average momentum is $\sim$ 300 MeV in accordance with expectation from ee → qq jet events measured at comparable values of W[33].

4. Search a $t\bar{t}$ threshold

Two approaches have been used in the past to search for a threshold of $t\bar{t}$ production at PETRA

a) a measurement of $R = \sigma_{had}/\sigma_{\mu\mu}$[34],

b) a measurement of the topology of the events at various center of mass energies[34,35].

In particular, a scan in cm energy steps of 20 MeV was performed between 29.9 and 31.46 GeV[36]. No indication for a $t\bar{t}$ bound state or anopen $t\bar{t}$ threshold has been found (assuming charge 2/3 t quarks). Details have been reported at this conference by W. Bartel.

The PLUTO group has applied a complementary method of searching for a $t\bar{t}$ threshold by measuring the rate of inclusive muons [5]. Provided the t quark decays dominantly via the t → b → c → s chain with a $\sim$ 10 % muonic branching ratio at each step we expect a drastic increase of inclusively produced muons above the $t\bar{t}$ threshold.

The analysis was performed with the outer muon identifier which consists of an equivalent of one meter of iron followed by a drift chamber system with a solid angle acceptance of 80 % of 4π. We observe 53 hadronic events with muon candidates having $p_\mu > 2$ GeV at cms energies of 27 - 31.6 GeV. The main sources of background are pion and kaon decay and hadronic punchthrough. After background subtraction a signal of 27 muon events is obtained. The results are summarized in table 7.

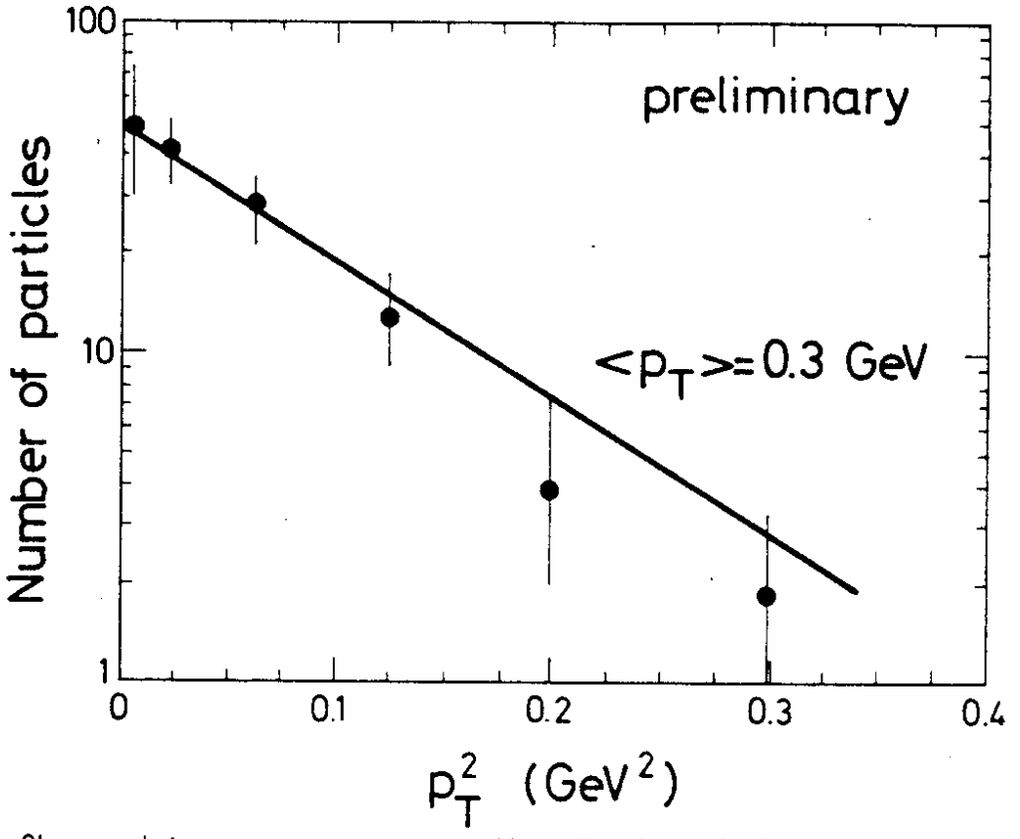

Fig. 13 Observed transverse momentum distribution of charged tracks from events $ee \to ee\,q\bar{q}$ measured relative to the jet axis

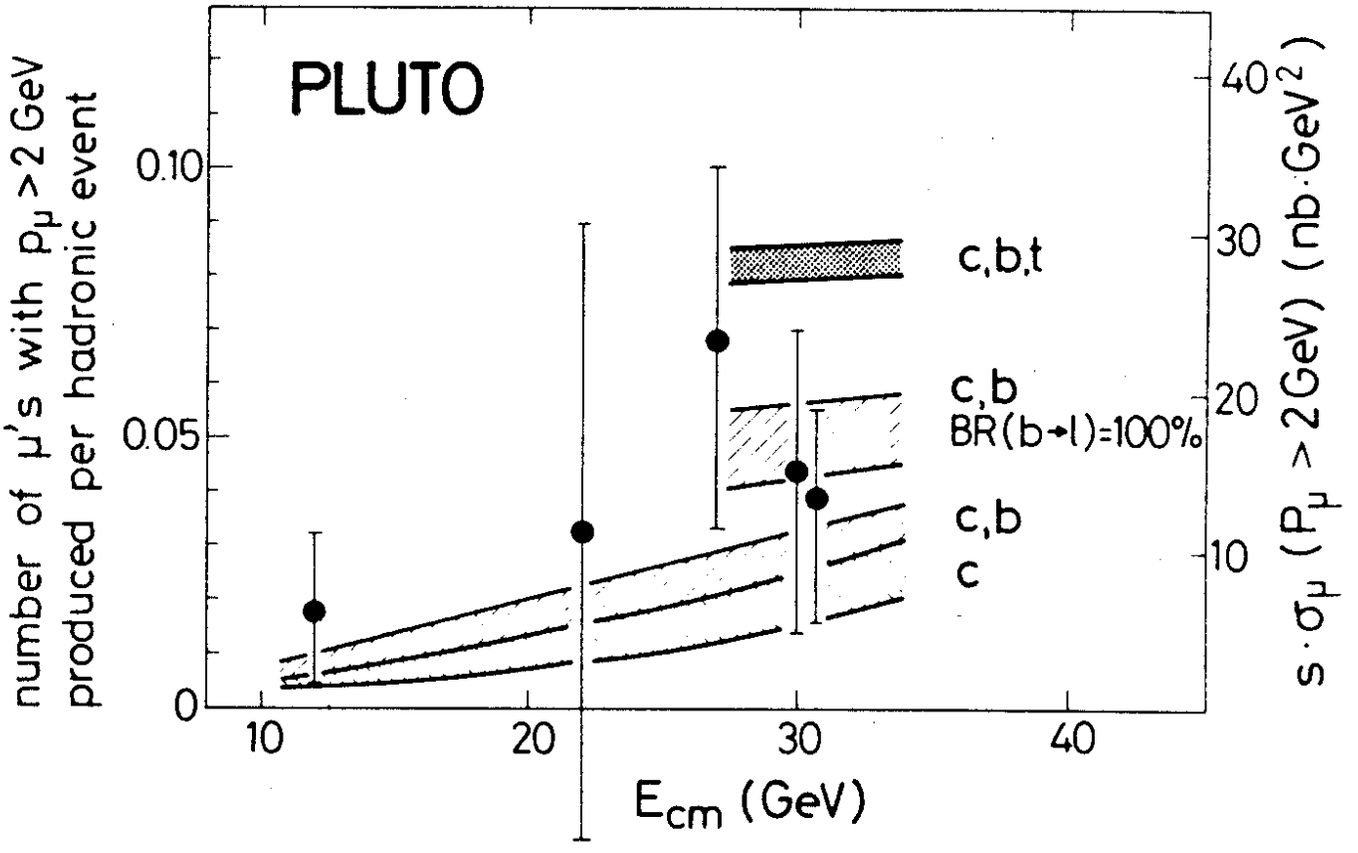

Fig. 14 The number of inclusive muons with $p_\mu > 2$ GeV produced per hadronic event, corrected for full geometric acceptance and identification efficiency. The shaded bands show the predictions of the four-, five- and six quark production model.

Table 7 Inclusive muon production (with $p_\mu > 2$ GeV/c). The results in columns 5 and 6 are corrected for acceptance, track reconstruction and muon identification efficiency.

$\sqrt{s}$ (GeV)	hadronic events	μ candidates	μ signal events	μ's per hadronic event (%)	$s \cdot \sigma_\mu$ (>2 GeV) (nb · GeV^2)
12.0	199	3	2.29	$183^{+1.39}_{-1.40}$	$6.2^{+4.8}_{-4.8}$
22.0	28	1	0.58	$3.30^{+5.69}_{-5.74}$	$11.2^{+19.3}_{-19.5}$
27.6	157	10	6.74	$6.82^{+3.26}_{-3.48}$	$23.2^{+11.6}_{-12.2}$
30.0	209	11	5.80	$4.41^{+2.60}_{-3.01}$	$15.0^{+9.0}_{-10.4}$
30.7	612	32	15.15	$3.94^{+1.61}_{-2.33}$	$13.3^{+5.8}_{-8.1}$
$\Sigma > 27$	978	53	27.70	$4.43^{+1.39}_{-2.35}$	$15.0^{+5.2}_{-7.6}$

We attribute the source of the muon events to the semi-leptonic decays of mesons containing heavy quarks c, b and possibly t. Monte Carlo simulations have been used to test various hypotheses. These simulations are based on the Field-Feynman two jet production model[37] modified to include heavy quarks, as described by Ali[38]. Assuming a heavy quark semi-leptonic branching ratio to muons of 10 % we have computed inclusive muon production with $p_\mu > 2$ GeV/c for the following 3 cases: i) the four-quark model, udsc, ii) the five-quark model, udscb, and iii) the six-quark model, udscbt. As a modification of the five-quark model we consider the possibility in case iv) that b mesons decay only semileptonically with equal branching ratios to electrons, muons and taus[39].

We have studied the sensitivity of these predictions to various assumptions such as the heavy quark masses, the quark fragmentation functions, the chirality of the quark weak decay couplings and the emission of gluons. The only significant variation arises from different assumptions concerning quark fragmentation. We therefore present the predicted muon signals as the shaded bands in fig. 14. The top edge of each band corresponds to the assumption of a constant fragmentation function, while the bottom edge corresponds to the standard Feynman-Field fragmentation for light quarks: $f(z) = 0.23 + 2.31 (1-z)^2$. As can be seen from fig. 14 our measurements are consistent with models i), ii) and iv) for the full range of fragmentation functions considered here.

The larger muon rate expected from the production of top mesons is ruled out by our measurements, which do not show the sharp increase in the muon signal which would be expected to set in abruptly at the top threshold.

Fig. 15 shows the momentum spectrum of the muons observed at center of mass energies above 27 GeV. Also shown are the predictions of models ii) and iii) for comparison. As can be seen our measurements are consistent with the shape of either predicted spectrum although in absolute magnitude they naturally reflect the same conclusions as can be drawn from the integral results.

We observe three opposite side dimuon events. This number is consistent with sources from background (0.67 ± 0.27), charm (0.38 ± 0.14) and bottom (0.50 ± 0.17) semi-leptonic decays. The additional number of opposite side dimuon events expected with the production of top is 3.14 ± 1.11.

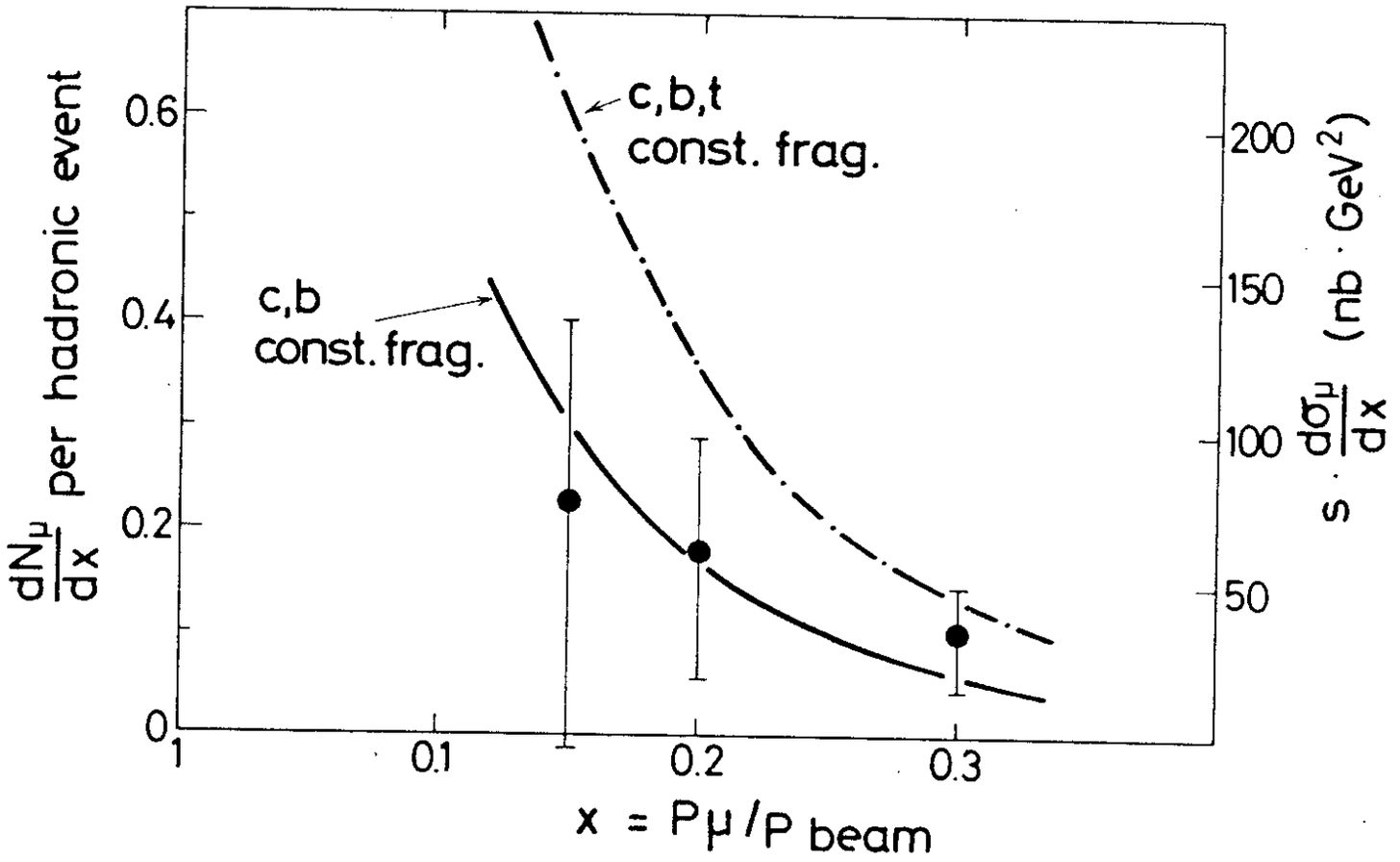

Fig. 15 The momentum spectrum $s \cdot d\sigma/dx$ of inclusive muons produced in hadronic events at cms energies from 27.6 to 31.6 GeV. The curves show predictions of the five- and six quark models assuming a constant fragmentation function for the c, b and t quarks.

5. Search for spin 0-leptons

Let me finally discuss a particle search performed with PLUTO. Although most present day e^+e^- experiments focus on questions relevant to the "standard" electroweak interactions and QCD, there is growing interest in the grand unification of electroweak and strong interactions and in supersymmetry which includes also gravitation. As discussed recently by G. Farrar and P. Fayet, supersymmetry implies that all particles have partners with spin differing by 1/2 unit[40]. In particular one expects two spin 0 partners of the electron, s_e and t_e corresponding to the left handed part and the right handed part of the Dirac lepton fields. In a special class of models their masses are expected to be $\leq$ 40 GeV[41].
When the energy is high enough, $s\bar{s}$ and $t\bar{t}$ pairs can be produced in e^+e^- annihilation via the following diagrams

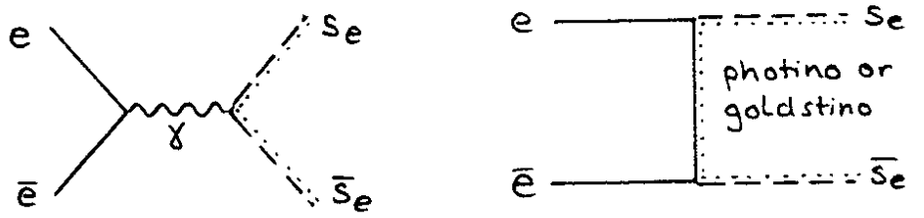

The first graph describes a regular one photon annihilation. In the second diagram a photino or a goldstino can be exchanged. Here, the photino is the spin 1/2 partner of the photon and the goldstino is the goldstone fermion associated with the spontaneous breaking of the supersymmetry. The diagrams for $t\bar{t}$ production are similar to the diagrams for $s\bar{s}$ production. The cross section for $s\bar{s}$ and $t\bar{t}$ production is given by[40]

$$\sigma\,(e^+e^- \to s_e\,\bar{s}_e + t_e\bar{t}_e) = \beta^3\,\frac{\sigma_{\mu\mu}}{4} + \text{corrections terms.}$$

The s_e particles decay via $s_e \to e^-$ + photino (goldstino) with a very short lifetime. The photino and goldstino are expected to interact neutrinolike. Thus the decay signature is a single electron, carrying part of the beam energy.
We have scanned our data for the following topologies

$$e^+e^- \to e^+e^- + \text{no photon shower},$$

where the electrons have an energy $> E_{beam}/5$ and are acoplanar by $> 15^0$. The acoplanarity cut removes coplanar events of the type ee → ee ee with two electrons emitted in the beam pipe.

We have 46 candidates in our 30 - 31.6 GeV data, but all events have an additional photon shower. Hence the signal is zero events. The detection efficiency is estimated to be 40 %. From the above information we derive a lower limit on the mass of spin 0 electrons of

$M(s_e, t_e) > 13$ GeV at 95 % c.l.

We have checked this results using electron pairs measured at lower center of mass energies by varying the acoplanarity cut.

6. Summary

Let me summarize the above results:

1) QED works well up to $|q^2|$, $s \approx 1000$ GeV^2 as shown in fig. 1 - 6 and table 4. The e, μ and τ behave as pointlike particles. Effects of the standard weak interactions are not yet detectable given the energies and event rates available in the last year.

2) We have studied $\gamma\gamma$ interactions as a source of
   - C = + resonances (fig. 8),
   - a hadronic continuum, where the photons interact dominantly hadronlike (figs. 9,10) and
   - pointlike interactions. In particular we have first evidence for large p_t jets from the process $\gamma\gamma \to q\bar{q}$ (figs. 11,12)

3) The inclusive μ spectra show no $t\bar{t}$ threshold up to center of mass energies of 30 GeV (figs. 13,14)

4) We have set a lower limit of 13 GeV (95 % c.l.) on the mass of spin 0 electrons expected from supersymmetry.

Acknowlegdment

I am indebted to my collegues of the PLUTO collaboration, who helped me in preparing this report. I thank V. Hepp, R. Kellogg, W. Wagner and G. Zech for a careful reading of the manuscript.

References

1. D. Schmidt, Proceedings of this conference
2. The present members of the PLUTO collaboration are:

   Ch. Berger, H. Genzel, R. Grigull, W. Lackas, F. Raupach
   I. Physikalisches Institut der RWTH Aachen, Germany

   A. Klovning, E. Lillestöl, E. Lillethun, J.A. Skard
   University of Bergen, Norway

   H. Ackermann, F. Barreiro, J. Bürger, L. Criegee, H.C. Dehne, A. Eskreys, G. Franke, W. Gabriel, Ch. Gerke, G. Knies, E. Lehmann, H.D. Mertiens, U. Michelsen, K.H. Pape, H.D. Reich, M. Scarr, B. Stella, U. Timm, W. Wagner, P. Waloschek, G.G. Winter, W. Zimmermann
   Deutsches Elektronen Synchrotron DESY, Hamburg, Germany

   O. Achterberg, L. Boesten, V. Hepp, H. Kapitza, B. Koppitz, B. Lewendel, W. Lührsen, R. van Staa, H. Spitzer
   II. Institut für Experimentalphysik der Universität Hamburg, Germany

   C.Y. Chang, R.G. Glasser, R.G. Kellogg, K.H. Lau, R.O. Polvado, B. Sechi-Zorn, A. Skuja, G. Welch, G.T. Zorn
   University of Maryland, College Park, USA

   A. Bäcker, S. Brandt, K. Derikum, A. Diekmann, C. Grupen, H.J. Meyer, B. Neumann, M. Rost, G. Zech
   Gesamthochschule Siegen, Germany

   H.J. Daum, H. Meyer, O. Meyer, M. Rössler, D. Schmidt
   Gesamthochschule Wuppertal, Germany

3. PLUTO collaboration, Ch. Berger et al., DESY report 80/01 and Zeitschrift für Physik C4 (1980) 269
4. PLUTO collaboration, Ch. Berger et al., Phys. Letters 89B (1980) 120
5. PLUTO collaboration, Ch. Berger et al., Inclusive muon production at PETRA energies, to be published.
6. J.E. Augustin et al., Phys. Rev. Letters 34 (1975) 233;
   T. Himel et al., Phys. Rev. Letters 41 (1978) 449
7. L.H. O'Neill et al., Phys. Rev. Letters 37 (1976) 395;
   B.L. Beron et al., Phys. Rev. D17 (1978) 2187 and 2839;
   E. Hilger et al., Phys. Rev. D15 (1977) 1809
8. a) T.D. Lee, G. Wick, Phys. Rev. D2 (1970) 1033,
   b) S.J. Brodsky, S. Drell, Ann. Rev. Nucl. Science 20 (1970) 147
   c) N.M. Kroll, Nuovo Cim. XLV (1966) 65
9. PLUTO collaboration, Ch. Berger et al., Measurement of the reaction $e^+e^- \to \gamma\gamma$ at cms energies from 9.4 to 31.6 GeV, to be published, DESY report 80/35
10. A. Litke, Ph. D. Thesis, Harvard University (1970), unpublished
11. J.A.M. Vermaseren, private communication

12. Ch. Berger, Proceedings of the 1979 International Conference on Two-Photon Interactions, Lake Tahoe (USA) 30.8.-1.9.1979, University of California at Davis press

13. PLUTO collaboration, Ch. Berger et al., Lepton and hadron pair production in two photon reactions, to be published, DESY report 80/34

14. A. Bramon, M. Greco, Lett. Nuovo Cimento 2 (1971) 522

15. D. Faiman, H.J. Lipkin, H.R. Rubinstein, Phys. Letters 59B (1979) 269

16. S.B. Berger, B.T. Feld, Phys. Rev. D8 (1973) 3875

17. V.M. Budnev, A.E. Kaloshin, Phys. Letters 86B (1979) 351

18. N. Levy, P. Singer, S. Toaff, Phys. Rev. D13 (1976) 2662

19. H. Kleinert, L.P. Staunton, P.M. Weisz, Nucl. Phys. B38 (1972) 87

20. B. Schrempp-Otto, F. Schrempp, T.F. Walsh, Phys. Letters B36 (1971) 463

21. B. Renner, Nucl. Phys. B30 (1971) 634

22. J. Babcock, J.L. Rosner, Phys. Rev. D14 (1976) 1286

23. M. Greco, Y. Srivastava, Nuovo Cimento 43A (1978) 88

24. G. Schierholz, K. Sundermeyer, Nucl. Phys. B40 (1972) 125

25. V.N. Novikov, S.I. Eidelman, Soviet Journal of Nuclear Physics 21 (1975) 529

26. G.M. Radutzkij, Soviet Journal of Nuclear Physics 8 (1969) 65

27. W. Wagner, Proc. of the XIVth Recontre de Moriond (1979), ed. by J. Tran Thanh Van

28. S.J. Brodsky, T. De Grand, J. Gunion, J. Weis , Phys. Rev. D19 (1979) 1418

29. T. Walsh, J. Physique C2 Suppl. 3 (1974)

30. M. Greco, Y. Srivastava, Nuovo Cimento 43A (1978) 88; See also the earlier work of S.J. Brodsky, F.E. Close, J.F. Gunion, Phys. Rev. D6 (1972) 177 and T.F. Walsh, P. Zerwas, Phys. Letters 44B (1973) 195

31. TASSO Collaboration, R. Brandelik et al., Phys. Letters 86B (1979) 243;
MARK J Collaboration, D.P. Barber et al., Phys. Rev. Letters 43 (1979) 830;
PLUTO Collaboration, Ch. Berger et al., Phys. Letters 86B (1979) 418;
JADE Collaboration, W. Bartel et al., DESY preprint 79/80 (1979)

32. L. Boesten, private communication

33. PLUTO collaboration, Ch. Berger et al., Phys. Letters 78B (1978) 176

34. PLUTO collaboration, Ch. Berger et al., Phys. Letters 86B (1979) 413;
TASSO collaboration, R. Brandelik et al., DESY report 79/75 (1979);
MARK J collaboration, D.P. Barber et al., MIT report 107 (1979);
JADE collaboration, W. Bartel et al., Phys. Letters 88B (1979) 171

35. TASSO collaboration, R. Brandelik et al., Z. Phys. C4 (1980) 87;
JADE collaboration, W. Bartel et al., DESY report 79/70

36. TASSO collaboration, R. Brandelik et al., Phys. Letters 88B (1979) 199;
PLUTO collaboration, Ch. Berger et al., DESY report 80/02;
JADE collaboration, W. Bartel et al., DESY report 80/04;
MARK J collaboration, D.P. Barber et al., MIT Lab. of Nucl. Science report 110 (1980)

37. R.D. Field, R.P. Feynman, Nucl. Phys. B136 (1978) 1

38. A. Ali, Z. Phys. C1 (1979) 25

39. See e.g. H. Georgi, M. Machacek, Phys. Rev. Letters 22 (1979) 1639 and references therein.

40. G.R. Farrar, P. Fayet, Phys. Letters 89P (1980) 191

41. P. Fayet, Phys. Letters 84B (1979) 416